Electronic Journal of Structural Engineering

Original Article

Cite this: DOI:10.56748/ejse.24765

Received Date: 24 February 2025
Accepted Date: 30 July 2025

1443-9255
https://ejsei.com/ejse

Identification and Damage Detection in Concrete Structures Based on Genetic Algorithm Combined with Cluster Analysis

Xukai Ren [a*], Ke Wang [b], Xiaofang Han [a], JingYi Zhang [a]

[a] School of Architecture and Engineering, Henan Technical Institute, Zhengzhou 450042, China
[b] School of Commerce, Henan Technical Institute, Zhengzhou 450042, China
*Corresponding author: rk13938230870@126.com

Abstract

With the advancement of the transportation industry, concrete structures are widely utilized in construction due to their benefits, including cost-effectiveness and ease of construction. To improve the accuracy of identification and damage detection in concrete structures, this study uses acoustic emission technology to obtain various waveform parameter features in the structure. It uses Back Propagation Neural Network (BPNN) to improve Genetic Algorithm (GA), while combining the K-means++ clustering analysis method for mixed damage identification. The results demonstrated that the model's accuracy in identifying the location of damage was as high as 98.46%, and the accuracy of identifying the degree of damage was 97.23%. In terms of Area Under Curve (AUC), the model achieved 0.986 with a misclassification rate of only 1.54%. In summary, the research on identification and damage detection in concrete structures based on GA combined with clustering analysis significantly improves the accuracy and reliability of concrete structure damage detection. This study provides a new technical means for health monitoring of concrete structures in engineering practice.

Keywords

Genetic algorithm, Cluster analysis, Concrete structure, Damage detection, Acoustic emission

1. Introduction

The rapid development of the national economy of China has led to the growing evolution of modern structures towards large-span, high-rise, and lightweight directions, and people have put forth higher demands for the performance of building materials (Liu et al., 2024). However, with the passage of time and the influence of the external environment, concrete structures are inevitably subject to various forms of damage, which seriously affects their integrity, bearing capacity, and reliability as critical infrastructure. Therefore, accurately and efficiently identifying and detecting damage in concrete structures has become the focus of current attention. At present, commonly used methods for detecting damage to concrete structures mainly include visual inspection, ultrasonic testing, and Acoustic Emission Technology (AET) (Ullah et al., 2023). AET is a non-destructive testing method based on monitoring the high-frequency elastic waves emitted by materials under stress (Wu et al., 2021). When concrete structures suffer from cracks, peeling, corrosion, and other damages, stress waves are generated inside the material and propagate to the structure surface in the form of Acoustic Emission Signals (AESs). By analyzing its characteristic parameters, including frequency, amplitude, and duration, the health status, damage type, and damage propagation can be determined. The advancement of computer technology and intelligent algorithms has led to an increasing number of researchers introducing artificial intelligence technology into Structural Health Monitoring (SHM). Genetic Algorithm (GA) is an optimization method that simulates natural selection and genetic mechanisms and can find the optima by simulating the process of biological evolution. Cluster analysis is an unsupervised learning method that can maximize the data similarity within the same category and minimize the similarity between various categories by dividing the dataset into multiple categories (Javadian et al., 2021). Therefore, in this context, this study innovatively utilizes GA and clustering analysis techniques to extract effective information from abundant, intricate AES data, improving the accuracy of concrete structure damage detection.

The study aims to improve the accuracy of damage detection in concrete structures, combining GA and K-means++ methods, and applying AET for real-time monitoring and evaluation of structural damage. AET, as an advanced tool for SHM, can accurately determine the health status of structures through waveform feature analysis. The innovation of this study lies in the combination of GA and clustering analysis methods, providing a more efficient and accurate solution for damage detection of concrete structures.

AET is often applied in Concrete Damage Detection (CDD) due to its high sensitivity, strong real-time performance, and non-destructive advantages, and has received attention from many experts and scholars. Thiele et al. designed a concrete damage evolution detection approach using AET combined with ultrasonic testing technology to analyze the fatigue process of concrete under Compressive Cyclic Loading (CCL). This method measured the strain, elastic modulus, and static strength of concrete under CCL through acoustic emission and ultrasonic signals, and was feasible (Thiele et al., 2022). Habib et al. developed a method that fuses AET with the K-Nearest Neighbor (KNN) algorithm to detect crack types. Their approach achieved an accuracy of 96.51% in crack classification. Other studies have also explored similar methods, with varying results on classification accuracy, highlighting the effectiveness of AET in this application (Habib et al., 2020). Van Steen et al. proposed using AET to obtain the acoustic emission source characteristics of chloride-induced corrosion damage in reinforced concrete to improve the accuracy of health monitoring of concrete structures. It combined the time-frequency characteristics provided by continuous wavelet transform to effectively distinguish the location of acoustic emission sources, significantly improving the accuracy of concrete structure health monitoring (Van et al., 2022). Li et al. proposed using AET for full load test acoustic emission energy analysis to monitor the damage status of reinforced concrete sewage pipelines. The study investigated the evolution trend of mechanical properties and acoustic emission monitoring indicators under load, effectively detecting the degree of damage and destruction of reinforced concrete sewage pipeline structures (Li et al., 2022).

GA plays an important role in damage identification and classification. Toma et al. suggested a hybrid motor current data-driven method to enhance the accuracy of motor bearing fault diagnosis. This method extracted statistical features from the motor current signal and used GA to reduce the quantity of features and choose the most vital ones. It effectively enhanced the precision of fault diagnosis (Toma et al., 2020). Alexandrino et al. constructed a CDD method that fuses Multi-objective GA (MOGA), neural network, and fuzzy decision-making to lift the accuracy of CDD. It utilized Back Propagation Neural Network (BPNN) to robustly optimize the damage detection model, effectively improving detection accuracy (Alexandrino et al., 2020). Civera et al. proposed an MOGA strategy based on robust optimal sensor placement to improve the accuracy of loss detection in building infrastructure engineering. This method placed sensors on building structures for signal collection and analyzed the signals through MOGA. This method could effectively detect potential damage to building structures (Civera et al., 2021). To address this limitation, unsupervised learning methods have gained attention for their ability to detect anomalies without prior labeling. Eltouny et al. proposed a Bayesian optimization unsupervised learning method to improve the performance of building SHM. This method combined density-based unsupervised learning and GA for damage localization and detection, with good potential and robustness in detecting and locating structural damage (Eltouny et al., 2021).

In summary, existing literature mostly uses AET and GA for damage detection, and some studies combine clustering analysis, such as Toma et al.'s research. This paper proposes combining improved GA and cluster analysis to enhance the accuracy and robustness of the model, maintaining high detection accuracy in different interference environments. This paper uses AEP monitoring and combines AEP analysis with improved GA to effectively identify deep or hidden damages such as crack propagation and interface delamination. In addition, existing research is mostly limited to detecting shallow surface damage or conducting experimental verification under specific conditions.

2. Identification and Damage Detection of Concrete Structures

This study first uses AET for CDD. The required waveform signal features are extracted through Acoustic Emission Parameter (AEP) analysis, and the damage is identified and classified using improved GA and clustering analysis methods.

2.1 Damage Identification in Concrete Structures Using AET

The widespread application of concrete structures in various engineering projects makes them susceptible to external loads and environmental changes during long-term use, resulting in various damages such as cracks, peeling, and corrosion. Traditional damage detection methods, such as visual inspection and ultrasonic testing, although able to detect surface or shallow damage to a certain extent, have significant limitations in detecting deep or concealed damage (Yuan et al., 2022). AET can monitor the propagation of stress waves inside the structure in real time, thereby capturing damage signals such as crack propagation and interface delamination inside the concrete (Kim et al., 2020). Therefore, this study utilizes AET to monitor the signals generated by the failure of concrete structures themselves. The detection principle of AET is displayed in Fig.1.

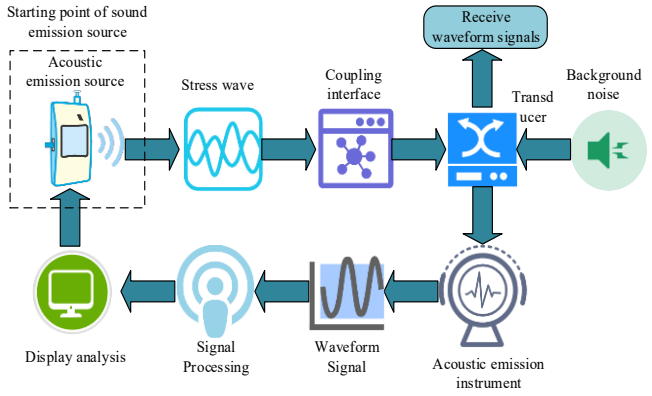

Fig.1 Principle of AET Testing

In Fig.1, firstly, the acoustic emission source is excited inside the tested material, generating stress waves that are transmitted to the surface of the structure through the coupling interface. After removing background noise through a transducer, the acoustic emission instrument captures waveform signals and processes, displays, and analyzes them. Acoustic emission sources generally propagate elastic waves in the propagation modes of transverse waves, longitudinal waves, and surface waves (Zou et al., 2022; Azimi et al., 2020). The calculation of transverse wave velocity is shown in equation (1).

$$v_t = \sqrt{\frac{E}{2\rho(1+\sigma)}} \tag{1}$$

In equation (1), v_t is the velocity of transverse waves, E means the elastic modulus, ρ denotes the density, and σ is the Poisson's ratio. The formula for longitudinal wave velocity is shown in equation (2).

$$v_l = \sqrt{\frac{E(1-\sigma)}{\rho(1-2\sigma)(1+\sigma)}} \tag{2}$$

In equation (2), v_l is the velocity of longitudinal waves. The expression for the amplitude of sound waves is shown in equation (3).

$$M = M_0 e^{-\varsigma d} \tag{3}$$

In equation (3), M means the amplitude of the acoustic emission wave. M_0 refers to the amplitude at the sound emission source. e corresponds to the base of the natural logarithm. ς denotes the attenuation coefficient. d is the propagation distance of acoustic emission waves in the material (Zhang et al., 2020). However, the amount of waveform signal data detected by AET from the tested material is very large. Therefore, it is needed to use AEP analysis methods for signal processing to extract feature parameters that can characterize damage information. The analysis of AEP is exhibited on Fig.2.

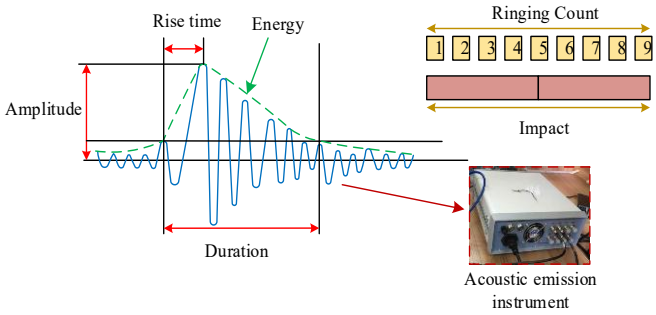

Fig.2 Analysis of Acoustic Emission Parameters

In Fig.2, multiple key features can be extracted from the waveform parameters of the AES, including ringing count, energy, amplitude, rise time, duration, etc. Among them, the threshold voltage, as the setting value for noise filtering, is usually set to 30 dB to ensure effective signal while removing environmental noise (Hebbi et al., 2023). In acoustic emission analysis, B-value is one of the commonly used parameters, particularly suitable for describing the characteristics of crack activity (Tibaduiza et al., 2020; Mangalathu et al., 2020). B-value is usually related to the energy and amplitude data of Acoustic Emission Events (AEE), used to reflect the different stages and mechanisms of crack propagation. Therefore, this study uses B-value as a parameter index for CDD, as shown in equation (4).

$$log_{10} N = A - BM \tag{4}$$

In equation (4), B is the CDD parameter index B-value, used to describe the energy distribution characteristics. A is a constant representing the overall activity of the AEE. N is the number of events with an amplitude $\geq M$. By calculating the B-value size, the activity characteristics of concrete cracking can be determined. A high B-value indicates a relatively stable cracking process, while a low B-value indicates that the cracks inside the structure are expanding more vigorously and are about to undergo instability and failure (Yilmaz et al., 2024). The formula for the damage variable D is given by equation (5).

$$D = \frac{S_f}{S_{cd}} \tag{5}$$

In equation (5), S_f is the loss area of concrete cracks, and S_{cd} is the damage area when the concrete completely fractures. The calculation of the number of AEEs N_S is given by equation (6).

$$N_S = \frac{N_{cd}}{S_{cd}} \tag{6}$$

In equation (6), N_{cd} is the cumulative number of AEEs during the complete fracture process of concrete. The stress level Y generated by them N_{cd} is shown in equation (7).

$$Y = \alpha N_{cd} + \beta\, ln(1 + \varepsilon N_{cd}) \tag{7}$$

In equation (7), α , β , and ε all represent the loss coefficients of the acoustic emission rate theory.

2.2 Damage Detection Model Based on Improved GA and Clustering Analysis

After collecting the signal characteristics of concrete structures through AET in this study, further processing and analysis of these signals are needed to achieve accurate damage identification and classification. Currently, common methods for damage identification of AESs mainly include feature extraction methods, clustering analysis methods, deep learning-based damage identification methods, and hybrid methods (Stepinac et al., 2020). To handle the constraints of a single method in practical applications, the paper combines the advantages of multiple methods and adopts a hybrid approach for damage identification. GA, as a commonly used method in deep learning-based damage recognition, has the advantages of strong global search capability, wide applicability, and good parallelism. However, traditional GA suffers from slow convergence speed, and it is easy to fall into local optima (Pan et al., 2020). Therefore, this study improves GA by introducing BPNN. BPNN can continuously adjust weights and thresholds through its three-layer network structure, thereby further refining the solution space based on global optimization. Fig.3 shows the BPNN structure.

In Fig.3, the BPNN structure includes layers of input, hidden, and output. The input layer receives candidate solutions from the GA optimization process and passes these signals to the hidden Layer. The hidden layer transforms the input signal through a nonlinear activation function to generate richer feature representations. The output layer calculates the final result of damage recognition or optimizes the objective function value based on the output of the hidden layer. Through the

backpropagation algorithm, BPNN can continuously adjust the weights and thresholds in the network based on the error between the output results and the actual target, thereby minimizing the error and optimizing the objective function. Therefore, combining BPNN with GA's global search capability can finely resolve space based on global optimization and improve the overall optimization effect. Fig.4 shows the model framework built on improved GA.

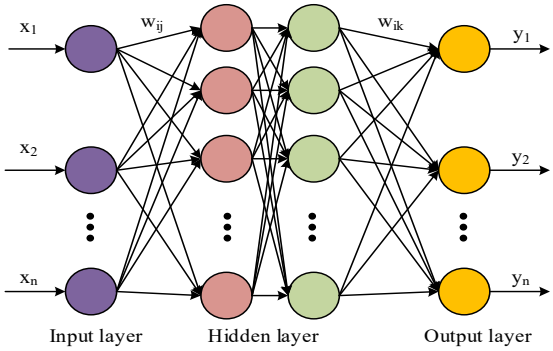

Fig.3 Diagram of BPNN

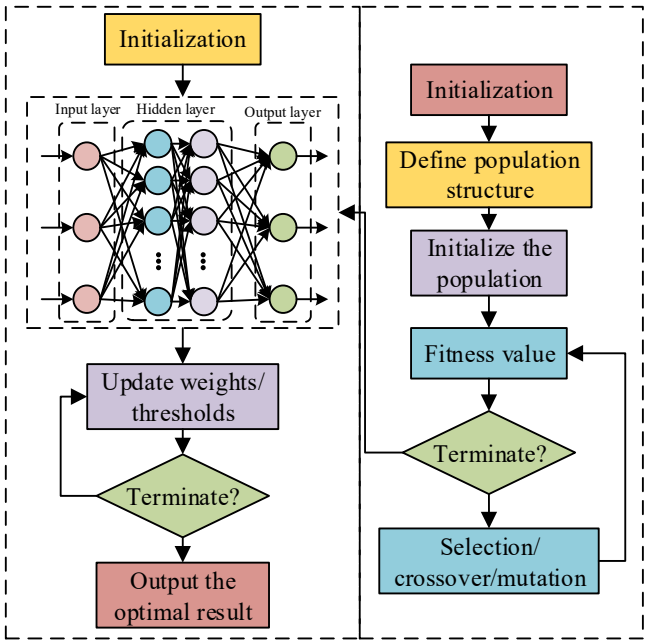

Fig.4 A Damage Detection Model Framework on the Basis of Improved GA

In Fig.4, in the model framework, the parameters of BPNN and GA are initialized first, and the population structure of GA is defined after randomly assigning weights and thresholds. The next step is to initialize the population configuration and calculate the fitness value of the initial population. By determining whether fitness meets the requirements for selection, crossover, mutation, and other operations, the optimal weights and thresholds are ultimately obtained and used as input data for the BPNN input layer. After adjusting the three-layer network structure of BPNN, the model can obtain the optimal result through judgment. The fitness value is shown in equation (8).

$$F = \tau\left(\sum_{i=1}^{n}\left|O_i - O_i^{'}\right|\right) \tag{8}$$

In equation (8), F is the fitness value, τ is the proportionality coefficient, n is the number of nodes, O_i and $O_i^{'}$ are the true and predicted outputs of the i -th node. The probability P_i of the i -th individual being selected is shown in equation (9).

$$P_i = \frac{F_i}{\sum_{j=1}^{m} F_j} \tag{9}$$

In equation (9), m is the gross of individuals. F_i and F_j are the fitness values of individuals i and j . The mathematical expression for crossover operation is shown in equation (10).

$$\begin{cases} a_{kj}^{'} = a_{kj} \times (1-\psi) + a_{ij} \times \psi \\ a_{ij}^{'} = a_{ij} \times (1-\psi) + a_{kj} \times \psi \end{cases} \tag{10}$$

In equation (10), $a_{kj}^{'}$ and $a_{ij}^{'}$ are the j -th gene value of the new individual $a_k^{'}$ and $a_i^{'}$. ψ is a random number within the [0,1]. The expression for the mutation operation is shown in equation (11).

$$\begin{cases} a_{ij} = a_{ij} + \left(a_{ij}^{max} - a_{ij}\right) \times \emptyset, r \geq 0.5 \\ a_{ij} = a_{ij} + \left(a_{ij}^{min} - a_{ij}\right) \times \emptyset, r < 0.5 \end{cases} \tag{11}$$

In equation (11), r is a random number and ϕ is the variation amplitude factor. a_{ij}^{max} and a_{ij}^{min} are the maximum and minimum of the gene j in the individual i. The mathematical formula for the variation amplitude factor is shown in equation (12) (Mariniello et al., 2021).

$$\phi = r\left(1 - \frac{g}{g_{max}}\right) \tag{12}$$

In equation (12), g and g_{max} are the current and maximum iterations. The K-means++ algorithm is widely utilized in clustering analysis methods for damage identification due to its good clustering effect. Therefore, this study adopts a hybrid method combining improved GA and the K-means++ algorithm for damage detection. To evaluate the clustering effect, this study uses the Silhouette Coefficient (SI) to measure the quality of clustering results, as shown in equation (13) (Salkhordeh et al., 2023).

$$SI(u) = \frac{\bar{d}_{x_u} - \bar{d}_{x_u,C_u}}{max\{\bar{d}_{x_u} - \bar{d}_{x_u,C_u}\}} \tag{13}$$

In equation (13), $SI(u)$ is the SI of the u -th data sample. $\bar{d}_{x_u}$ and $\bar{d}_{x_u,C_u}$ are the average distance from sample point x_u and x_u to all other points in its cluster and cluster C_u. The formula for the Davies-Bouldin Index (DBI) is shown in equation (14).

$$DBI = \frac{1}{y}\sum_{u=1}^{y} \underset{v \neq u}{max}\left(\frac{R_u - R_v}{d_{uv}}\right) \tag{14}$$

In equation (14). R_u and R_v are the radii of clusters u and v . y is the number of clusters. d_{uv} is the distance between u and v (Luo et al., 2022). The clustering radius can represent the radius and degree of dispersion of the cluster, as shown in equation (15).

$$R_{C_u} = \left\{\frac{1}{|C_u|}\sum_{x_u \in C_u}\left|x_u - x_{C_v}\right|^q\right\}^{\frac{1}{q}} \tag{15}$$

In equation (15), R_{C_u} is the degree of dispersion of cluster C_u. q is the index of distance measurement, and the smaller the value of R_{C_u} , the better the clustering effect. By combining improved GA and k-means++, the accuracy and efficiency of damage identification can be effectively improved, thereby achieving more efficient and reliable SHM. To improve recognition accuracy, this paper has made improvements based on traditional GA, adopting fitness function optimization and cross-mutation strategy, increasing local search ability, and enhancing the algorithm's global optimal solution ability. Combining the K-means++ clustering analysis method can maintain high clustering performance and low misclassification rate on large-scale datasets.

3. Performance Verification of identification and damage detection in concrete structures methods

After setting up the experimental environment, this study first verified the recognition performance of concrete structures based on AET and then analyzed the damage detection models built on improved GA and clustering analysis.

3.1 Experimental Platform Setup and Environment Configuration

An acoustic emission sensor model from Physical Acoustics Corporation is selected for signal acquisition to verify the performance of the identification and damage detection in concrete structures methods. A high-performance computing platform equipped with an Intel i7 processor, 32GB RAM, and 1TB SSD is used for data processing, and MATLAB software is used for model training. LabVIEW software is used to control the data acquisition system and sensors and monitor experimental data in real-time. PyTorch is used as a deep learning framework for data processing and neural network training.

To further verify the robustness of the proposed identification and damage detection in concrete structures method in complex environments, a confusion experiment is designed to test the model's performance under these conditions by introducing different types of interference factors. These experiments aim to simulate various environmental noises and interferences in practical applications, ensuring that the model can maintain efficient and stable performance even in complex backgrounds. To simulate noise interference in actual environments, different types of background noise are introduced in the experiment, including vibration noise, electronic noise, and electromagnetic interference. The introduction of noise is achieved by adding external vibration sources and electromagnetic interference equipment to the experimental site, simulating the noise conditions in common industrial environments. Confusion experiment steps: Firstly, an acoustic emission sensor is used to collect signals, and the AESs in the

concrete structure under different interference conditions are recorded. By introducing interference such as background noise, the training model identifies different types of damage under these conditions. Finally, by calculating the confusion matrix of the model in various interference environments, the accuracy of damage detection in different types of damage recognition is evaluated. Table 1 lists the specific configuration.

Table 1. Experimental Environment Configuration

Category	Device	Model
Data Acquisition Equipment	Acoustic Emission Sensor	Physical Acoustics Corporation
	Data Acquisition Card	National Instruments (NI) PCI-6115
Computing Platform	Computer	Intel i7/32GB RAM/1TB SSD
Software Tools	MATLAB	R2023b
	Programming Language	Python 3.8+
	Deep Learning Framework	PyTorch 1.8
	Development Environment	2019LabVIEW
Power Supply Equipment	Power Supply Unit	EPS-4000

3.2 Performance Verification of Concrete Structure Identification Based on AET

To verify the effectiveness of AET in identifying concrete structures, this study selects ordinary concrete specimens with dimensions of 100mm×100mm×300mm and subjects them to continuous stress treatment. The surface of the test piece is equipped with a Physical Acoustics Corporation model acoustic emission sensor for signal acquisition. The study applies continuous stress to concrete specimens and observes the changes in AES parameter characteristics. In Fig.5 (a), as external stress grows, the amplitude of the AES shows a trend of first increasing, then stabilizing, and then decreasing. In the first 65 seconds, the amplitude gradually increases, and between 65 seconds and 300 seconds, the amplitude remains stable, while after 300 seconds, the amplitude significantly decreases. AET can effectively reflect the dynamic changes of concrete structures during the stress process. In Fig.5 (b), the trend of energy change is also similar to the amplitude change, showing a slow increase in energy in the early phase, with a stable trend in the middle phase and a sharp decrease in the later stage. This state further confirms the AET's accuracy in identifying changes in concrete structures.

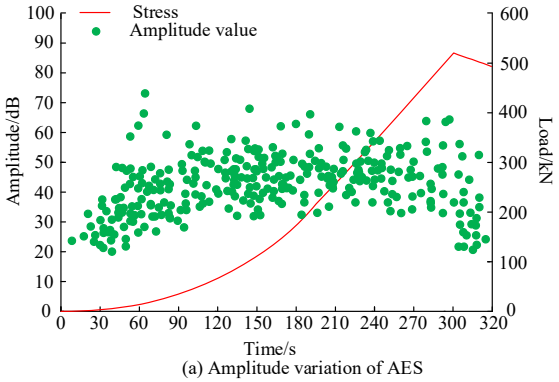

(a) Amplitude variation of AES

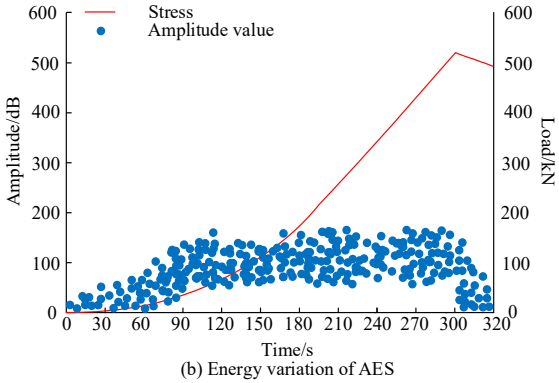

(b) Energy variation of AES

Fig.5 Changes in Parameter Characteristics of AES

To further analyze the crack propagation in concrete structures, the changes of concrete specimens before and after crack formation are studied and observed. The crack propagation in concrete structures is shown on Fig.6. Before the formation of cracks, the internal structure of the concrete component is intact, and no obvious cracks are observed. After the formation of cracks, penetrating cracks appear inside the concrete components, further indicating the damage evolution process of concrete under external stress.


(a) Concrete component diagram before crack formation


(b) Diagram of concrete components after crack formation

Fig.6 Crack propagation diagram of concrete structure

To further measure the effectiveness of the concrete structure identification method built on AET, the changes in B-value under different stress types, such as compressive stress (ranging from 0 to 50 MPa) and tensile stress (ranging from 0 to 20 MPa), are compared. In Fig.7 (a), under low stress, the B-value shows a slow decreasing trend over time, decreasing from the initial 3.12 to 2.98. This indicates that under low stress, the damage process of concrete structures is relatively slow, and crack propagation is relatively stable. In Fig.7 (b), under high stress, the B-value starts from 3.12 and decreases to 3.01 after 75 seconds of variation. Between the 75 s and the 95 s, the decrease in B-value significantly increases. Between 95s and 100s, the B-value sharply decreases and eventually drops to 1.23. Under high stress, the crack propagation speed in concrete structures accelerates, and the instability process of the structure gradually becomes apparent. In summary, the change in B-value can effectively demonstrate the propagation of cracks and the instability process of structures. This change is compared with the real crack formation and propagation data obtained from visual and displacement measurements. Additionally, other quantitative measurements, such as strain gauges and crack width monitoring, are also used to further validate the AET accuracy in identifying concrete structure damage.

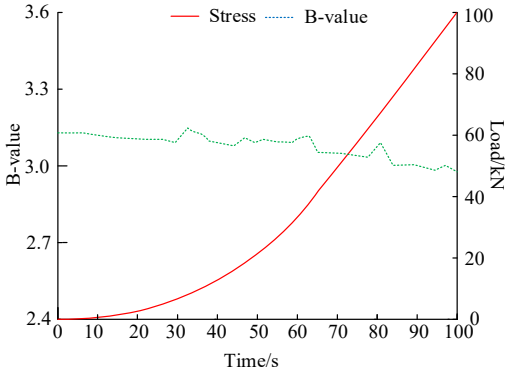

(a) Changes in B-value under small stress

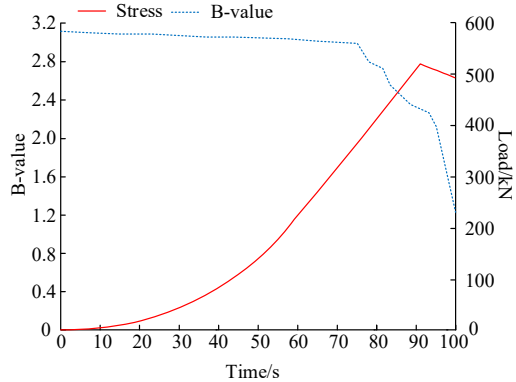

(b) Changes in B-value under high stress

Fig.7 Changes in B-value under Different Stress Conditions

To test the effectiveness of this recognition method in practical applications, the study collects parameter changes that gradually increase

with external loads in different actual engineering environments, as shown in Table 2. The variation trends of amplitude, B-value, and energy of AESs are consistent in different engineering environments. Taking the experimental group of concrete bridges as an example, as the external road slowly rises, the amplitude of the AES rises from 0.5 to 2.1. This indicates that as the load increases, micro-cracks and defects inside the concrete are gradually activated, leading to an enhancement of AESs. In addition, the B-value decreases from 3.1 to 2.2, reflecting the acceleration of the crack propagation process. The energy change from 0.2 to 0.8 indicates that energy consumption gradually increases with the increase of load. The actual dynamic changes are measured through crack width monitoring and strain gauges and compared with the variations in AES parameters. The crack width increases from 0.1 mm to 0.5 mm, and the strain increases from 0.2% to 1.5%. The consistency between the measured dynamic changes and AES trends provides empirical evidence for the effectiveness of identification technology in practical applications.

Table 2. Parameter Changes in Different Practical Engineering Environments

Engineering environment	Time/s	Amplitude	B-value	Energy
Concrete bridge	0	0.5	3.1	0.2
	50	1.2	2.95	0.5
	100	2.3	2.7	1.0
	150	2.8	2.5	1.3
	200	2.1	2.2	0.8
Concrete floor slab	0	0.8	3.15	0.3
	50	1.5	2.95	0.6
	100	2.4	2.7	1.0
	150	3.1	2.5	1.4
	200	2.8	2.4	1.2
Concrete dam	0	1.1	3.05	0.4
	50	2.2	2.9	0.8
	100	3.5	2.7	1.1
	150	4.0	2.5	1.5
	200	3.1	2.2	1.2

3.3 Performance Verification of Damage Detection Model on the Basis of Improved GA and Clustering Analysis

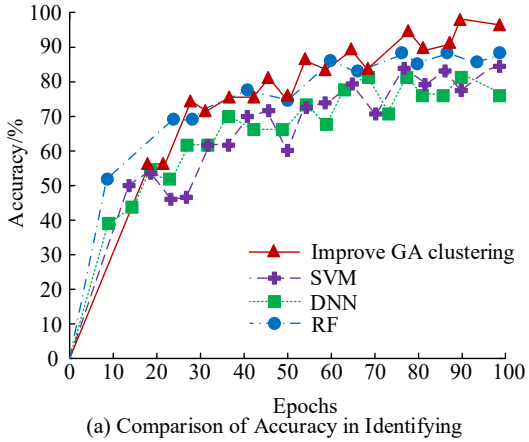

(a) Comparison of Accuracy in Identifying Damage Locations

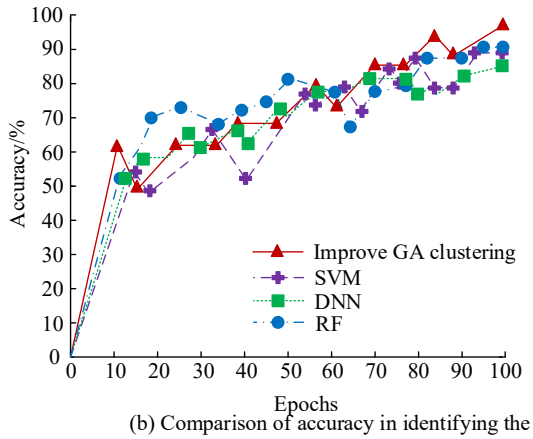

(b) Comparison of accuracy in identifying the degree of damage

Fig.8 Comparison of Accuracy of Different Damage Detection Models

To verify the proposed model, this study compares the model with three other advanced algorithms, namely Support Vector Machine (SVM), Deep Neural Network (DNN), and Random Forest (RF). Fig.8 shows the accuracy of various models. In Fig.8 (a), the accuracy of the research model in damage location recognition is as high as 98.46%, which is 12.64%, 15.83%, and 10.42% higher than the 85.82%, 82.63%, and 88.04% of SVM, DNN, and RF models, respectively. In Fig.8 (b), the accuracy of the research model in identifying the degree of damage is 97.23%, which is 8.15%, 11.23%, and 7.69% higher than 89.08%, 85.00%, and 90.54% of other models. Overall, the research model has excellent performance in damage detection.

To further validate the performance, the comprehensive performance of different models is compared in three experiments. In Table 3, the comprehensive performance indicators of the research model are significantly better than those of models. The precision, recall, and F1-Score of the research model reach 97.12%, 96.78%, and 96.95%, while the performance of other models in these three indicators does not exceed 90%. In terms of AUC, the value of the research model is as high as 0.986, which is 10.66%, 13.07%, and 7.75% higher than the comparison model. Additionally, the computation time of the research model is only slightly 2.2 seconds longer than that of the SVM model, which still has an advantage in computation time compared to DNN and RF. The Misclassification Rate (MCR) of the research model is only 1.54%, while the MCRs of other models are all greater than 10%. In the second and third experiments, the research model also demonstrates superior performance, with accuracies of 97.20% and 97.05%. The average precision of the three experiments is as high as 97.12%. The average recall rate and F1-Score are 96.81% and 96.87%, indicating that the research model maintains a high level of performance under different experimental conditions. In summary, the research model has demonstrated superior performance in damage detection.

Table 3. Comprehensive Performance of Four Models

The number of experiments	Index	Improved GA clustering	SVM	DNN	RF
1	Precision/%	97.12	83.50	81.87	87.32
	Recall/%	96.78	84.92	80.45	88.67
	F1-Score/%	96.95	84.21	81.15	87.00
	AUC	0.986	0.891	0.872	0.915
	Calculation time/s	20.5	18.3	31.4	25.6
	MCR/%	1.54	14.18	17.37	11.96
2	Precision/%	97.20	83.74	81.90	87.40
	Recall/%	96.71	84.35	80.85	88.22
	F1-Score/%	96.83	83.11	81.89	87.25
	AUC	0.987	0.895	0.875	0.901
	Calculation time/s	20.3	18.2	31.5	25.6
	MCR/%	1.52	14.2	17.0	11.81
3	Precision/%	97.05	83.92	81.80	87.52
	Recall/%	96.95	84.42	80.89	88.20
	F1-Score/%	96.84	83.25	81.11	87.36
	AUC	0.983	0.891	0.872	0.911
	Calculation time/s	20.7	18.2	31.6	25.70
	MCR/%	1.51	14.25	17.30	11.95

To verify the clustering performance, this study compares it with other advanced clustering algorithms. The selected algorithms include K-means, hierarchical clustering, and Density-Based Spatial Clustering of Applications with Noise (DBSCAN). Fig.9 shows the performance comparison of different clustering methods. In Fig.9 (a), the SI value of the improved GA clustering method used is as high as 0.98, while the SI values of K-means clustering, hierarchical clustering, and DBSCAN are 0.87, 0.79, and 0.93. The SI values of the research method increased by 11.22%, 19.38%, and 5.10% compared to other methods. In Fig.9 (b), the DBI value of the research method is the lowest, only 0.24, which is 70.73%, 59.32%, and 47.82% lower than the 0.82, 0.59, and 0.46 values of other models. The research model has significantly better clustering performance than other clustering algorithms.

To verify the performance of the model in practical applications, this study evaluates its performance in different scenarios through confusion experiments. In Fig.10 (a), the correct recognition probability is higher than 0.94 for different types of injuries. The correct identification probabilities of damage types such as cracks, corrosion, fatigue, and wear reach 0.98, 0.95, 0.94, and 0.96. In Fig.10 (b), the damage detection accuracy outperforms 0.91 under different environmental noise interferences. Under complex environmental conditions such as vibration, temperature changes, electronic interference, and electromagnetic interference, the damage detection accuracy of the model still remains at

0.93, 0.92, 0.91, and 0.92. The research model has high efficiency and stability under different types of damage and interference environments.

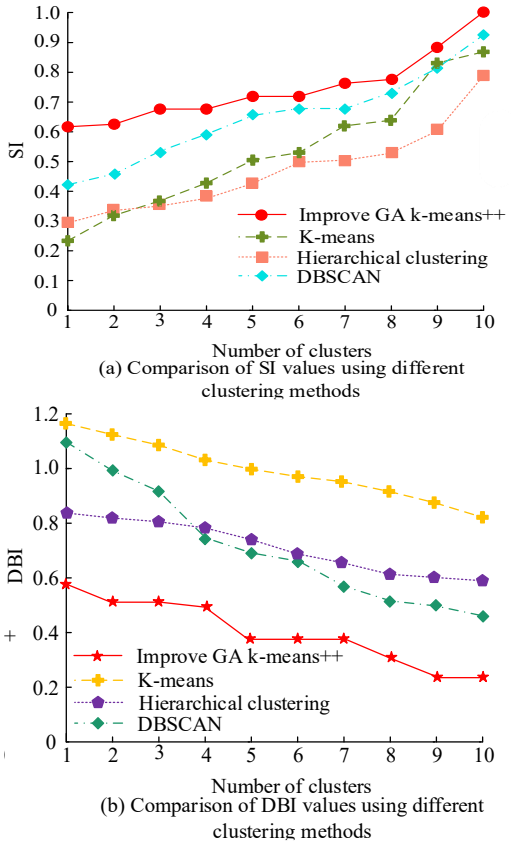

(a) Comparison of SI values using different clustering methods

(b) Comparison of DBI values using different clustering methods

Fig.9 Performance Comparison of Different Clustering Methods

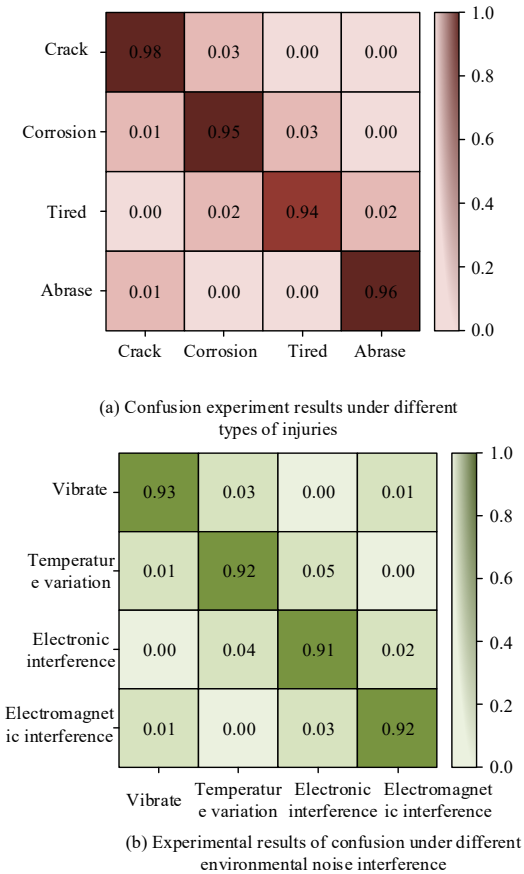

(a) Confusion experiment results under different types of injuries

(b) Experimental results of confusion under different environmental noise interference

Fig.10 Confusion Experiment

4. Conclusions

Health monitoring and damage detection of concrete structures have always been important topics in the engineering field. To optimize the accuracy of damage detection in concrete structures, this study adopted an improved GA combined with clustering analysis technology to identify and detect concrete damage by analyzing the variation law of AEP data. AET could effectively capture damaged information of concrete structures and accurately display the dynamic changes of concrete structures. The accuracy of the research model in identifying the location and degree of damage exceeded 98%, significantly better than other advanced models. In the comprehensive performance assessment, the precision, recall, and F1-Scores of the research model reached 97.12%, 96.78%, and 96.95%, with an AUC value of 0.986 and an MCR of only 1.54%. In addition, the improved GA clustering method also performed well in clustering performance, with SI values and DBI of 0.98 and 0.24, obviously better than other clustering methods. In the confusion experiment, the correct recognition probability under different types of damage was higher than 0.94, and the damage detection accuracy under different environmental noise interferences was higher than 0.91. In summary, the proposed concrete structure damage detection method based on GA and cluster analysis improves the accuracy and reliability of detection and provides a new technical means for SHM in practical engineering. Future research can further integrate deep learning techniques to enhance the adaptability of models in complex environments and explore the identification of more types of structural damage.

Although this method has achieved good results in experimental environments, there are still some limitations in current research, one of which is model simplification. Especially when dealing with complex situations that may be encountered in practical engineering, simplified assumptions may not fully reflect the true structural behavior. For example, the research model did not fully consider the dynamic response and damage accumulation process of concrete structures under earthquake or other extreme loads. This may result in different application effects in practical engineering compared to laboratory environments, especially when evaluating seismic performance. Simplified models may not fully reflect the behavior of concrete structures under earthquake action.

Funding

The research is supported by 2023 Henan Province Key Research and Promotion Special Project (Science and Technology Tackle), CPS Network Internal Decision Model and Key Technology Research for Building Structure Health Monitoring (Project Number: 232102210087).

References

Liu J, Jiang C, Yang X, & Sun, S. Review of the application of acoustic emission technology in green manufacturing. International Journal of Precision Engineering and Manufacturing-Green Technology, 2024, 11(3): 995-1016. https://doi.org/10.1007/s40684-023-00557-w

Ullah N, Ahmed Z, Kim J M. Pipeline leakage detection using acoustic emission and machine learning algorithms. Sensors, 2023, 23(6): 3226-3230. https://doi.org/10.3390/s23063226

Wu X, Yan Q, Hedayat A, & Wang, X. The influence of concrete aggregate particle size on acoustic emission wave attenuation. Scientific Reports, 2021, 11(1): 22685-22689. https://doi.org/10.1038/s41598-021-02234-x

Javadian Kootanaee A, Hosseini Shirvani M. A hybrid model based on machine learning and genetic algorithm for detecting fraud in financial statements. Journal of Optimization in Industrial Engineering, 2021, 31(2): 169-172.

Thiele M, Pirskawetz S. Analysis of damage evolution in concrete under fatigue loading by acoustic emission and ultrasonic testing. Materials, 2022, 15(1): 341-348. https://doi.org/10.3390/ma15010341

Habib M A, Kim C H, Kim J M. A crack characterization method for reinforced concrete beams using an acoustic emission technique. Applied Sciences, 2020, 10(21): 7918-7922. https://doi.org/10.3390/app10217918

Van Steen C, Nasser H, Verstrynge E, & Wevers, M. Acoustic emission source characterisation of chloride-induced corrosion damage in reinforced concrete. Structural Health Monitoring, 2022, 21(3): 1266-1286. https://doi.org/10.1177/14759217211013324

Li P, Zhang W, Ye Z, Wang, Y., Yang, S., & Wang, L. Analysis of acoustic emission energy from reinforced concrete sewage pipeline under full-scale loading test. Applied Sciences, 2022, 12(17): 8624-8631. https://doi.org/10.3390/app12178624

Toma R N, Prosvirin A E, Kim J M. Bearing fault diagnosis of induction motors using a genetic algorithm and machine learning classifiers. Sensors, 2020, 20(7): 1884-1887. https://doi.org/10.3390/s20071884

Alexandrino P S L, Gomes G F, Cunha Jr S S. A robust optimization for damage detection using multiobjective genetic algorithm, neural network and fuzzy decision making. Inverse Problems in Science and Engineering, 2020, 28(1): 21-46. https://doi.org/10.1080/17415977.2019.1583225

Civera M, Pecorelli M L, Ceravolo R, Surace, C., & Zanotti Fragonara, L. A multi-objective genetic algorithm strategy for robust optimal sensor placement. Computer-Aided Civil and Infrastructure Engineering, 2021, 36(9): 1185-1202. https://doi.org/10.1111/mice.12646

Eltouny K A, Liang X. Bayesian-optimized unsupervised learning approach for structural damage detection. Computer-Aided Civil and Infrastructure Engineering, 2021, 36(10): 1249-1269. https://doi.org/10.1111/mice.12680

Yuan C, Xiong B, Li X, Sang, X., & Kong, Q. A novel intelligent inspection robot with deep stereo vision for three-dimensional concrete damage detection and quantification. Structural health monitoring, 2022, 21(3): 788-802. https://doi.org/10.1177/14759217211010238

Pan X, Yang T Y. Postdisaster image-based damage detection and repair cost estimation of reinforced concrete buildings using dual convolutional neural networks. Computer-Aided Civil and Infrastructure Engineering, 2020, 35(5): 495-510. https://doi.org/10.1111/mice.12549

Kim B, Cho S. Automated multiple concrete damage detection using instance segmentation deep learning model. Applied Sciences, 2020, 10(22): 8008-8011. https://doi.org/10.3390/app10228008

Zou D, Zhang M, Bai Z, Liu, T., Zhou, A., Wang, X., ... & Zhang, S. Multicategory damage detection and safety assessment of post-earthquake reinforced concrete structures using deep learning. Computer-Aided Civil and Infrastructure Engineering, 2022, 37(9): 1188-1204. https://doi.org/10.1111/mice.12815

Azimi M, Eslamlou A D, Pekcan G. Data-driven structural health monitoring and damage detection through deep learning: State-of-the-art review. Sensors, 2020, 20(10): 2778-2781. https://doi.org/10.3390/s20102778

Zhang C, Chang C, Jamshidi M. Concrete bridge surface damage detection using a single-stage detector. Computer-Aided Civil and Infrastructure Engineering, 2020, 35(4): 389-409. https://doi.org/10.1111/mice.12500

Hebbi C, Mamatha H. Comprehensive Dataset Building and Recognition of Isolated Handwritten Kannada Characters Using Machine Learning Models. Artificial Intelligence and Applications, 2023, 1(3):179-190. https://doi.org/10.47852/bonviewAIA3202624

Tibaduiza Burgos D A, Gomez Vargas R C, Pedraza C, Agis, D & Pozo, F. Damage identification in structural health monitoring: A brief review from its implementation to the use of data-driven applications. Sensors, 2020, 20(3): 733-742. https://doi.org/10.3390/s20030733

Mangalathu S, Sun H, Nweke C C, Yi, Z., & Burton, H. V. Classifying earthquake damage to buildings using machine learning. Earthquake Spectra, 2020, 36(1): 183-208. https://doi.org/10.1177/8755293019878137

Yilmaz Z, OKUR F Y, GÜNAYDIN M, & ALTUNIŞIK, A. C. Modal participation ratio in damage identification of building structures: A numerical validation. Journal of Vibration and Control, 2024, 30(15-16): 3269-3283. https://doi.org/10.1177/10775463231196952

Stepinac M, Gašparović M. A review of emerging technologies for an assessment of safety and seismic vulnerability and damage detection of existing masonry structures. Applied sciences, 2020, 10(15): 5060-5068. https://doi.org/10.3390/app10155060

Luo J, Huang M, Lei Y. Temperature effect on vibration properties and vibration-based damage identification of bridge structures: A literature review. Buildings, 2022, 12(8): 1209-1213. https://doi.org/10.3390/buildings12081209

Mariniello G, Pastore T, Menna C, Festa, P & Asprone, D. Structural damage detection and localization using decision tree ensemble and vibration data. Computer-Aided Civil and Infrastructure Engineering, 2021, 36(9): 1129-1149. https://doi.org/10.1111/mice.12633

Salkhordeh M, Mirtaheri M, Rabiee N, Govahi, E., & Soroushian, S. A rapid machine learning-based damage detection technique for detecting local damages in reinforced concrete bridges. Journal of Earthquake Engineering, 2023, 27(16): 4705-4738. https://doi.org/10.1080/13632469.2023.2193277

Disclaimer